Gold mobility within dune systems on the Barns property, Wudinna, South Australia: a partial extraction approach.

Liam. B. McEntegart*.

CRC-LEME, Geology & Geophysics, School of Earth and Environmental Science, The University of Adelaide, Adelaide 5005

*Corresponding Author: Fax +61883034347

Email liam.mc_entegart@student.adelaide.edu.au

Table of Contents

Abstract

Regolith carbonate is an established sampling medium in Au exploration. It has a demonstrated correlation with Au content in south western Australia, and was the prime indicator in the discovery of the Barns Au prospect Eyre Peninsula, South Australia. Whole rock ICP-MS, AAS and XRF analyses on samples from regolith drill cores and a trench cut into an aeolian sand dune on the Barns prospect established a correlation of Au content (≤17 ppb) with Ca, K, Al and Mg. XRD whole rock and mineral-separate analyses identified calcite, smectite and ankerite/dolomite as the main authigenic mineral phases present in the dune sand. The range of Sr isotope ratios of regolith carbonate ($^{87}Sr/^{86}Sr$ = 0.716234±16) and bedrock ($^{87}Sr/^{86}Sr$ = 0.731205±15) samples and their systematic variation imply that the Sr (and Ca) in the authigenic minerals was derived from a combination of surface ($^{87}Sr/^{86}Sr_{SMOW}$ = 0.709) and bedrock sources ($^{87}Sr/^{86}Sr$ = 0.731205±15). Sequential extraction, designed to determine gold fractionation between the authigenic mineral phases showed that Au is most prominently extracted from a Fe-Mn oxide phase while dissolution of carbonate does not necessarily mobilise the Au.

Keywords

Gold, calcrete, regolith carbonate, sequential extraction, particle size separation, Sr isotopes, Barns gold prospect.

Introduction

The soils of Australia mirror the great age of the continent. This is dictated by the latitude and climate, consequently much weathering has occurred over the years. Considering that glaciation in the Pleistocene was restricted to the south east, there has been no orogenic movement since the late Jurassic and tectonics were restricted to shearing, faulting and

vertical uplift, the land form of Australia has been altered while still allowing for older landforms and weathered products to persist (Beckman, 1983). As a result of this and the aforementioned climate, erosional material in the recent past has been transported only a minimal distance from source and formed the extensive alluvial plains and aeolian dunes we see today within Australia (Beckman, 1983).

The extensive regolith cover overlying bedrock hampers exploration within Australia. This regolith overburden can interact with underlying geology and take on some properties of the mineralogy and chemical composition of the rocks beneath. Regolith geology and especially geochemistry has provided useful tools for exploration, in particular the Au - Ca relationship within regolith carbonates, or calcrete, has lead to several successes in the discovery of significant Au mineralisation in the underlying bedrock. Study in the Mt Hope area (Lintern, 1989) was the first to show a direct relationship between Au and calcite (calcrete) which suggested that Au may be mobilized within soils and precipitated during the soil-carbonate formation process. Instead of acting as a diluent to Au, as it does with Fe and various other chemical components, calcrete may concentrate free Au in soils and thus provides a sampling medium for exploration.

Location & Geology

The Barns Au exploration target is located approximately 25 km north of Wudinna on the Northern Eyre Peninsula, S.A. situated within the southern Gawler Craton, which underlies the greater part of central South Australia. The Gawler Craton is defined as the region of Archaean to Mesoproterozoic crystalline basement that has undergone no substantial deformation, except for minor brittle faulting, since 1450 Ma (Thomson, 1975). The Gawler Craton consists of a Late Archaean to Paleoproterozoic basement that is

surrounded by Palaeoproterozoic to Mesoproterozoic orogenic belts (Daly et al., 1998). The recorded history of the craton shows several cycles of magmatism, sedimentation and orogenesis (Daly et al. 1998). The major complexes in the Archaean are the Sleafordian and Mulgathing complexes, both recorded within the Gawler Craton as highly deformed supracrustal successions (Daly and Fanning, 1993).

Situated on farming land the Barns area is easily accessible due to cleared natural vegetation and road access (Figure 1). Newcrest mining in 1996 initially discovered the Barns Au anomaly after a regional calcrete sampling. Sample spacing of 1km discovered anomalous Au values over the Barns region. In 1999 Adelaide Resources completed check sampling and obtained the exploration license from Newcrest after they had decided to give it up, focussing on more promising targets in NSW. Further calcrete sampling at 400, 200 and 100 m infill resulted in discovery of a 49 ppb Au peak with several significant values over 10ppb. Following a 50 hole RAB drilling program in which the final hole intersected two zones of mineralisation (8 m @2.97 g/t at 35 m depth and 7 m @ 1.80 g/t at 69 m depth). Further drill holes have encountered anomalous values for Au in the bedrock and geochemical drilling programs during 2000 defined three main mineralised zones with a combined strike length of approximately 1.2 km (Drown, 2003). Au values from mineralised drill hole intersections range from 2 m @ 67.6 g/t to 32 m@ 1.05 g/t

The following summary of the *in-situ* geology of the Wudinna area has been adapted from Drown, (2003). The eastern part of the Barns prospect is part of the metamorphic Archaean Sleaford Complex, the west is dominated by intrusives of the 1690-1680 Ma Tunkillia Suite (Ferris et al., 2002). Mafic granulites, felsic paragneisses and rare carbonate/magnetite rich units form the majority of the Sleaford Complex. The intrusive

Tunkillia suite includes moderately to strongly deformed granodioritic gneisses, which outcrop just to the northeast of the Barns Deposit. The area contains the Gawler Range Volcanics (GRV) and the Hiltaba suite intrusives dated at 1590Ma (Daly et al., 1998). The presence of miarolitic cavities and also the proximity of the extrusive GRV to the Hiltaba Suite suggests that the formation of this unit was at shallow crustal levels (Drown, 2003). The Yarlbrinda shear zone located northwest of Barns is a Proterozoic transcrustal lineament that is overprinted by intrusions of the Koondoolka Pluton of the Hiltaba Granitoid intrusion (Daly et al., 1998; McLean and Betts, 2003). All of the geology of the area has been interpreted from drill core, government acquired geophysical data and geochronological data due to extensive cover by Quaternary sediments and consequently only limited outcrop.

The outline of the anomalies at Barns and the nearby Baggy Green follow a general northwesterly trend, broadly parallel to the Proterozoic Yarlbrinda shear zone. Anomalous Au content is continuous into the saprolite underlying the aeolian sands and extends into the fresh bedrock. Primary mineralogy of the underlying granodioritic bedrock that hosts the mineralisation consists of plagioclase, K-feldspar phenocrysts, quartz and biotite. Apatite, allanite, magnetite and zircon make up some of the accessory minerals all being identified from drilling in 2003 (Drown, 2003). The age of the granite which hosts the mineralisation has not been determined yet but it is assumed from visual inspection that the granite is similar to the 1680 Ma Tunkilla Suite granitoids occurring in the central Gawler Craton. These granitoids contain significant blocks of quartzite and gneissic country rock of unknown location ranging in size up to several hundred metres. Intruding into the above lithologies are mafic dykes of up to 5 m thicknesses that dip westerly. It is therefore assumed that the mineralisation and the dyke intrusion are interrelated and the shape and

orientation of the intrusive dykes was controlled by pre-existing structures (Drown, 2003). Au occurs in numerous, narrow, northwest dipping quartz-sulphide veins that are associated with extensive hydrothermal alteration, which have been locally altered to chlorite-sericite-pyrite mineral assemblages.

The area of the Barns prospect is extensively covered by regolith, dominated by deeply weathered bedrock and wind blown aeolian dune systems. The dune systems at Barns generally trend north westerly and range in size of up to 6m height, the majority being only 2-3 m high and appear to have an island-like appearance within the surrounding farmland. Spacing between the individual dunes ranges from 20 to 200 m with some dunes showing greater erosion than others. These Quaternary dune systems at Barns cover the mineralisation in the bedrock with a maximum thickness of up to 6 m. The Barns Au-anomaly is developed in calcrete-bearing regolith of the (or within) aeolian dunes. Carbonate rich zones vary with depth throughout the profile and as determined in previous studies (Drown, 2003; Schmidt Mumm and Reith, 2004) Au relates to carbonate and correlates well with the Ca content of the calcrete-bearing dune sands.

The aims of this project are to investigate the identified Au in carbonate anomaly with respect to the distribution of major and trace elements and to identify the mineralogical composition of carbonate bearing regolith in the aeolian cover on the Barns prospect. Selected samples were used to develop a sequential extraction method to investigate the distribution of Au in authigenic carbonates and clay minerals in the transported regolith. Results from this project will hopefully establish further understanding of the relationships of Au within the aeolian dune profile at the Barns prospect with respect to chemical and mineralogical processes. With further understanding of mobility, fixation and

concentration of trace metals within carbonates situated on the Barns prospect, calcrete as a sampling medium can be used as a "blue print" for further exploration for gold and trace metals within Australia in areas of similar regolith cover.

Sampling and Analytical Methods

Samples of various types of calcrete and calcareous sand were taken from the aeolian sand dunes using a percussion soil corer to provide regolith cores of 32 mm diameter from a depth down to approximately 4 m. The drill hole was placed at the boundary of a 6 m high aeolian dune and surrounding farmland approximately in the centre of the Barns property (see Figure 1). Samples were taken with soil corer lined with a PVC tube to keep the core samples intact and to allow onsite samples to be taken for measuring soil pH and conductivity at varying depths. The pH and conductivity were measured using a portable pH and conductivity meter and the method described follows closely to that detailed in Rayment & Higginson (1992). One part soil and 4 parts water were combined in a disposable plastic tube capped and then shaken for 2 minutes and left to settle for 15 minutes. The resulting pH and conductivity values cannot represent absolute values but provide a reliable relative indication for the trend of pH and conductivity in the different sample media. Further samples were taken from vertical and horizontal profiles on both the eastern and western walls of an approximately 6 m long trench cut transverse to a dune by PIRSA on the Barns property (see Figure 1 for location). These samples were selected after initial results from the first drill holes gave us targets to aim for. The regolith samples were analysed for whole rock composition by X- Ray Fluorescence (XRF) for major element composition and by commercially available partial digest, Atomic Adsorption Spectroscopy and Optical Emission Spectroscopy by commercial providers (GENALYSIS Ltd.) specialising in calcrete rock analysis.

Samples were analysed by XRF for major and trace elements to determine the composition, compositional range and variation of the material from the aeolian deposits. The analytical procedure was adapted from Elburg & Foden (1998) and Potts (1992). After weighing into alumina crucibles, dried sample was ignited overnight at 960°C to determine the loss on ignition comprising organic material, CO_2 from carbonates and possible volatiles. Nominally 1 g of ignited sample is weighed with nominally 4 g 12:22 flux (35.3% lithium-tetraborate and 67.7% lithium metaborate). The sample-flux mixture was then fused using a propane-oxygen flame at approximately 1150°C. For trace elements 5-10 g is added to 1ml polyvinyl alcohol and pressed into a pellet and dried at 60°C for 2 hours. Analysis were carried out on a Philips PW 1480 fluorescence spectrometer using an Sc-Mo X-ray tube operating at 40 kV and 75 mA. International standards are analysed to determine the detection limits, which vary from 1-5 ppm (±5 at 100xDL) for trace elements and ±5% for major elements.

The <2 μm grain size fraction was separated from the bulk quartz sand for determination of the mineral composition through X-ray Diffraction (XRD) as described in Moore & Reynolds (1989) following the observation that the >2 μm size fraction consists mainly of quartz sand. Samples were mixed with water and shaken to separate clay minerals then a 1 μm and further 2 μm, centrifuge separation followed by ethanol wash to assist quick drying of the separated sample. A small amount of <2 μm material is used for an XRD disk and the rest is washed with acetic acid to remove carbonates, then washed and dried again. Orientated XRD and XRF disks are prepared using 120 mg of sample mixed with 6 ml water, 4ml being added to the XRF and 2 ml to the XRD papers, respectively, followed by $BaCl_2$ & H_2O for XRF and $MgCl_2$, H_2O and glycerol. Data was analysed using the

SIROQUANT program, which analyses XRD data statistically and compares results to a general database of minerals. The software uses Bragg-Brentano geometry calibration curves, which is essential where strong low-angle XRD peaks are present. SIROQUANT allows Rietveld analysis using a unique program structure and comparison of results to over 300 mineral profiles stored in the programs database (Sietronics, 2004).

Based on the results of the XRD and XRF analyses, a sequential extraction method was designed to further determine the distribution of Au within the different mineral and size fractions. The selected sample (BNS54) was chosen for its homogeneous distribution of Au content of 14±2 ppb determined in several sample splits, suggesting that Au was present in non-particulate form and evenly distributed throughout the sample. The total Au content was considered high enough for the sequential extraction procedure. Approximately 1 kg of sample was split into 3 parts following the previously described method and the extraction was carried out on the bulk sample and separates of >2 μm and <2 μm size fractions respectively. After the grain size separation each fraction was split into 6 even sized samples each to undergo the respective steps of the extraction procedure. After each step the remaining residue was analysed for major and trace elements and Au. The design of the extraction procedure was adapted from previous work (Gray et al., 1999; Tessier, et al., 1979) while trying to implement simple techniques that can be widely used.

Step	Extraction Procedure
1.	Addition of 20 ml 1 M $CaCl_2$ and 1 M Acetic acid twice to selectively remove a Mg-carbonate (dolomite) fraction. The chemical properties of dolomite cause it to preferentially dissolve in the Ca saturated solution while the calcite fraction will remain relatively undissolved.

2. Addition of 20 ml 1 M $MgCl_2$ and 1 M acetic acid to preferentially remove the calcite fraction in analogy to STEP 1
3. Wash with 20 ml 1 M acetic acid 4 times to completely remove all carbonates
4. Addition of 0.5 M-hydroxylamine hydrochloride and 0.5 M HCl to remove Fe-oxides and Mn-oxides by reduction.
5. Finally 4 M HCl was added to the sample to remove crystalline Fe-oxides.

After each process step the residual sample was washed and dried and analysed for Au, Ag, Al, As, Ba, Bi, Ca, Co, Cr, Cu, K, La, Mg, Mn, Mo, Na, Ni, P, Pb, Rb, Sr, Te, Th, Ti, U, V, W, Yb, Zn & Zr.

Finally selected samples were analysed for their Sr^{87}/Sr^{86} ratio to deduce possible sources of the Ca of the regolith carbonate in the profile. These samples were taken from various sites including vertical and horizontal profiles as well as weathered saprolite from below the profile and from drill holes in mineralised weathered granite and fresh rock. The following method was adapted from Foden *et al*. (1995) however some slight amendments were made due to the ease in which these samples dissolve. Sample material was digested overnight in a 15ml Teflon PFA® vial using a combination of 4ml 50%w/w HF and 2ml 6M HNO_3 acids. This procedure was repeated after drying of the residue, followed by digestion of dried sample by 6M HCl to remove fluorides. Following the digestion the sample material was dissolved in 1.5ml 2M HCl and centrifuged to ensure separation of insoluble material. 1ml sample was taken and pipetted into cation exchange columns containing BioRad – AG50W – X8 (200-400mesh) and following different strengths of HCl addition, a Sr concentrate was collected. The resulting residue was re-digested in HCl and put through the cation exchange columns again and finally dried for loading onto

single Te filaments for the mass spectrometer. All analyses were carried out using the Finnigan MAT 262 Mass Spectrometer with all samples being run as metals. The Sr ratio was normalised to $^{88}Sr/^{86}Sr = 8.375209$ and during the experimental procedure the standard SRM ran constantly at 0.710260 ± 10 (2σ). Blanks collected after the first and second runs through the cation exchange columns returned values of 2ng and 9ng respectively which combined is below 0.1% of the total sample weight and is therefore insignificant in the determination of the $^{87}Sr/^{86}Sr$ isotope ratio.

Results

Results of the soil pH and conductivity measurements taken during fieldwork are shown in Figure 2. Conductivity and pH have a good relationship with a distinct increase at a depth of 1.5m. It must be noted that pH has a change in magnitude being shown as a log scale compared to conductivity. Comparison with Au concentration in the same horizon shows distinct relationships between the three species further suggesting the relationship of Au to regolith carbonate formation.

General geochemical trends in the calcrete bearing regolith

Major and trace element X-ray fluorescence (XRF), Aqua Regia Digest - Inductively Coupled Plasma Mass Spectrometry (ICP-MS) and Optical Emission Spectroscopy (OES) analyses show a consistent positive correlation down hole of Au with Ca and Mg but also K and Al (see Figure 3a). This Au – Ca correlation ranges from 3ppb Au / 1790ppm Ca at surface level to 18ppb Au / 49421ppm Ca at a depth of 2m. The relationship confirmed the results from previous studies (Drown, 2003; Schmidt Mumm and Reith, 2004) of a reliable and predictable variation of gold and calcium in the area. Other relationships seen in the

down hole data include a negative correlation of Au with Ni to depth and a reliable co-variation of Au and Ti

Initial analyses indicated a strong correlation between Au and K giving rise to thoughts of clay mineral involvement within the profile. The <2μm grain size fraction was separated according to the routines described by Moore and Reynolds (1989), the grain size separation was carried out to remove the dominance of quartz within the XRD pattern. Findings for this are displayed in Table 1a; quantitative estimates of the mineral content as inferred using SIROQUANT (Sietronics, 2004) are listed in Table 1b. The total amount of <2μm grain size fraction systematically increased with depth in the drill core. The predominant clay minerals identified in the samples were kaolinite ranging from 1.38-wt% at 0.3m to 7.59-wt% at 1.95m depth and smectite in the form of montmorillonite ranging from 1.09-wt% at 0.3m to 9.14-wt% at 1.95m depth (see Table 1b). Carbonate content in the samples could not be quantified, as the removal of carbonates is required before orientated samples for clay can be analysed. However, the XRD spectra derived before carbonate removal show strong domination by a calcite and ankerite phase. The peak for ankerite within the spectra is strongly shifted to the Mg side of ankerite and could be considered as dolomite.

The trench location in Figure 1 had three profiles analysed for major elements. Both the vertical profiles (Figure 4a&c) and the horizontal profiles (Figure4b) results are displayed in the corresponding figures. The sample profile results from the eastern face (Figure 5) were summarised to get a more consistent image of the compositional variation within the dune. Geochemistry from the trench further supports the positive relationships of Au with

Al, K, Ca and Mg as outlined for the drill core samples and also with Cu, all increasing in concentration with depth.

Along the walls of the trench dug into the aeolian dune four compositional zones could be distinguished upon visual inspection (from top to bottom, see also Figure 5):

Organic-rich root zone

The top 10-20 cm contain Spinifex grass roots and abundant organic detritus from trees and shrubs.

Depleted Zone

Ranging in thickness from 1.5 – 3 m depending on the location in the dune this zone is highly leached of elements and consists of almost white quartz sand with only minor, local root zones from the bigger trees enriched in organic matter. It is visibly distinct from the zones above and below.

Enrichment Zone

Visibly seen in the trench as an orange coloured horizon this zone is enriched in the elements leached from the upper zones. This zone is transitional between the Depleted Zone above and the Carbonate Zone below, showing intermittent relationships between the characteristics of these two zones.

Carbonate Zone

Two distinct types of carbonate occur: a fine powdery form that is dispersed throughout this zone and a stronger, cemented powder zone that forms around root zones penetrating to depth.

Figure 6a shows the elements relationships of the vertical profile on the eastern face of the trench. These results reiterate the patterns of element distribution as determined in drill

hole 1. However unlike in hole 1 Fe and Al increase from surface to Mineral Enrichment Zone but then decrease from the top of the enrichment zone downward. Samples taken from carbonate enriched root zones in the profile and adjacent low-carbonate sand show distinct compositional differences. Au is clearly enriched in the root zones characterised by high CaO and MgO contents. Each zone of root growth has extensive carbonate production surrounding it and this carbonate-rich zone is also highly enriched in Au as shown in Figure 6b.

Sequential extraction

The extraction procedure described previously illustrated by Figure 8 a & b must be normalised so comparison between individual splits can be made. The reasoning behind this is that the concentrations obtained from analyses represents only the concentration within that small sample. To compare these results the mass was converted back to the whole sample using the percentage of each sample weighed after each extraction technique. The result obtained from analysis (X_{Res}) was multiplied by the final weight (W_F) or recovered residue and divided by the original weight of the sample (W_i) before extraction. For example: -

$$\left[\left(W_F * X_{Res} \right) \Big/ W_i \right] = X_{Normalised}$$

$$\left[\left(77.4 * 15.354 \right) \Big/ 26.536 \right] = 44.8\, ppb$$

The <2μm fraction shows distinct Ca and Mg depletion indicating that some calcite and dolomite has been depleted from the sample however Au is enriched minimally K, Cu and Al are depleted slightly and Zr remains unchanged. Mn is depleted about half of the original amount although not as strongly as when dissolving the Mn oxides in step 4. After

step 2 Mg and Ca are again depleted Ca much more so than Mg highlighting the increased resistance to dissolve that dolomite has to calcite, however in this step Au is dissolved much less than when removing dolomite in step 1. The other elements under analysis only vary slightly in their concentrations after this extraction step. Step 3 attempts to remove the carbonate completely however as shown in the results only about half the total Ca, Mg and Mn is depleted. Elemental concentrations within this step are concurrent with the changes seen in step 1 and 2. Step 4 of the process removed a large portion of the Mn and Fe oxides and most importantly the major change in Au concentration occurs within this step as Au changes from 47 ppb to 28 ppb. Na, Mg, Ca and Mn all are depleted to about 50% the original sample while Zr, Al, and K remain relatively unchanged. The final step removed Mg and Ca completely while removing approximately 60% Mn and approximately 80% Na, the remaining elements are slightly depleted however not in the same amount as step 4.

Step 1 of the >2μm stream of the extraction shows large depletion of Ca, Mg, Mn and Na, with approximately 90%, 60%, 50% and 50% respectively. Au, Al, K and Zr are all relatively undissolved by the acetic acid. Step 2 had less impact with 60% of Ca and 20% of each Mg, Na and Mn being removed. K, Al, Zr and Au remain undissolved. Step three resulted in elemental concentration changes being greater than those shown in step 1 and 2 for Mn, Mg, Ca and Na, again the remaining elements remained relatively unchanged. Step 4 did not have as much effect on Mn, Mg, Ca and Na as 3 did depleting slightly less of each respective element. The final step totally removed Ca and most Mg, while strongly removing Na and Mn but not totally. Throughout the extraction Au was stable as was Zr and Al however K did reduce moderately after step 4.

The main variations throughout the extraction occurred in the Mn/Fe oxide removal step 4, which in the <2 μm stream removed 40% of the Au, this was followed by step 5 removing 15% and dolomite removal lead to approximately 7% of Au being removed. Within the >2μm stream Au was removed very little and even after step 5 the concentration changed very little in the sample. As suspected the strongest removal of calcite and dolomite occurred in step 5 however there is no real apparent correlation of Au to Ca/Mg removal.

Sr isotopic variation

Sr as an element can readily substitute for Ca within mineral structure due to their similar atomic radius 1.18 Angstroms and 1.00 Angstroms respectively and ionic charge; this leads to its use as an identifier for sources of calcium. There can also be replacement of K^{+} by Sr^{2+} within silica-based minerals when Al^{3+} replaces Si^{4+} (Capo et al., 1997). ^{87}Sr is augmented over geological time by the decay of ^{87}Rb with the half-life 48.8 billion years and using the ratio of radiogenic ^{87}Sr to naturally occurring ^{86}Sr sources for calcium can be found (Stewart et al., 1997). The isotopic ratio ($^{87}Sr/^{86}Sr$) for recent wind blown sources (Seaspray) of Sr can be assumed to be that of recent seawater at about 0.709. Once ratios have been defined then it is possible to use Sr as a tracer for sources of Ca as well as telling us about weathering relationships.

Different samples were analysed and the $^{87}Sr/^{86}Sr$ ratios found were high at the surface of the dune as well as within weathered granite beneath the profile. Mineralogy of these samples from whole rock analyses shows the dominant Ca bearing mineral to be calcite so results from Sr isotope analyses from whole rock dissolution can be assumed to be representative of the carbonate fraction. Fresh granite gave a ratio of $^{87}Sr/^{86}Sr$ = 0.731205±15 while carbonate rich zones lower within the trench profile gave results

ranging from 0.716234±16 at the edge to 0.711949±13 4m in from the southern edge (see Table 2). Several values lie distinctly outside the normal values for $^{87}Sr/^{86}Sr$. These were determined for the Organic Rich Root Zone of the dune at values of $^{87}Sr/^{86}Sr$ =1.004037±130, weathered granite from drill core revealed $^{87}Sr/^{86}Sr$ =1.068547±16 and the saprolite below the dune had a value of $^{87}Sr/^{86}Sr$ = 0.767059±13 (see Table 2 and Figure 5). An observation is that from the edge of the dune inward the Sr ratio slowly decreases from 0.7162 to 0.7119 following the height of the enrichment zone (approximately 2.5 m from surface) however at greater depth of 3.5 m the ratio is up to 0.715379±12.

Discussion of Results

General geochemical trends in the calcrete bearing regolith

Results from the project elemental analysis and clay mineral XRD have shown that apart from the well established correlation of Au with Ca and Mg, Au also shows a distinct co-variation with K throughout the sampled drill hole and dune profiles. The mineralogical identification of the K source was shown to be fine-grained authigenic smectite and kaolinite, in particular in samples deeper in the profile. The increase of smectite/kaolinite concentration through the profile is related to the K and Al within the profiles. This relationship is also reflected in the samples taken from the Enrichment Zone of the trench (see Figure 4c). However as shown in Figure 3 the correlation between MgO, CaO and Au is much stronger than that demonstrated for Al_2O_3 and K_2O, suggesting that Au is more strongly related to the carbonate forming process. At high concentrations of CaO, MgO and K_2O, the correlation with Au follows a linear trend for K_2O, whereas with respect to

MgO and CaO the trend follows an exponential pattern (see Figure 3b). This could be interpreted as demonstrating a gradual accumulation of Au with authigenic smectite and kaolinite but a more closely linked accumulation through (co-) precipitation of Au and carbonate. The exponential relationship of CaO and MgO to Au implies that the precipitation of carbonates scavenges available Au from the (under saturated) mineral forming solution but as carbonate precipitation is more intense, the amounts of available Au are insufficient to maintain a steady increase of Au concentration in carbonate. As a result the carbonate/Au ratio decreases. In a similar manner this process also affects the formation of authigenic smectites. It is at this stage where carbonate is formed that expands to CaO/Au ratios beyond the observed correlation prevailing at low Au and CaO concentrations. Thus the solution is exceeding its capacity to provide Au and creates an exponential type relationship in precipitation.

Field observations and chemical analyses can be used to identify mineralogical and chemical zoning within the dune structure (Figure 5). Reduced metal content within the Depleted Zone and the gradual accumulation of clay minerals and consequently enrichment of metals (especially Al and K) with depth, cumulating in the highest contents in the Enriched Zone suggest secondary transport and deposition of matter and authigenic mineral growth and not a lateritic weathering environment. If the clay minerals were simply deposited as aeolian clay layers the dunes would be expected to have an internal, primary stratification. The increase of metal content with depth rather suggests a combination of processes being involved: firstly the physical depletion of fine grained aeolian clays from the upper regions (Depositional Zone) of the dune and the subsequent accumulation lower in the profile (illuviation). Secondly, field observations and the

identified chemical and mineralogical relationships between upper and lower regions of the profile suggest that there is authigenic mineral growth of mainly carbonates and smectites.

Figure 7 shows results from both dune trench and drill hole 1 to illustrate the relative changes in element concentration from surface to depth for key elements. The data plotted along the x-axis represent the most recent material from the top of the profile. All other samples from depth profiles are plotted along the y-axis. The diagram thus shows variation of composition to depth with respect to the top sample. Following the assumption that deposition of material on the top surface was homogeneous through time, the variation of elements can be interpreted to represent post-depositional processes. Thus within the drill hole the strongest enrichment in Mg, Ca, Au, Al and K occurs 1.5-2 m from the surface systematically increasing with depth (aside from the contaminated sample). A decrease in SiO_2 amount and concurrent enrichment of Ca & Mg suggests that there is secondary mineral growth changing the concentration of the SiO_2. This is supported by the field observations, which showed authigenic mineral growth in the trench profiles. Figure 7b shows the vertical trench profile (see Figure 5 for location); however, in this case the deepest sample (3.25 m) is not the most enriched. The Enrichment Zone described previously lies from 2.2 m onwards however the strongest enrichment is in the upper layers, as elemental concentrations decrease after the initial concentration (see also Figure 6). Al, K and Zr are most enriched in the sample located at 2.2 m compared to Ca and Au, which are most concentrated at 2.75 m and Mg, which is at 3.25 m from the surface. Figure 6 shows that once the initial enrichment zone is reached Fe and Al decrease with depth. This relationship is understood for Fe as generally we know that calcrete has reverse concentration effects. (Lintern 1997). Al however could be reduced with depth after

reaching the enrichment zone because the major source for Al is wind blown clays and they concentrate in the upper enrichment zone.

The formation of the carbonate within the regolith is dependent on the availability of CO_2 and Ca or Mg (Lintern, 1997). There are three predominant sources of calcium: aeolian blown clay minerals, rainfall derived seaspray / seawater Ca or Ca input through weathering and leaching of the bedrock. We can assume that Ca is abundant in the (granitic) bedrock and mobilised through weathering. Roots from trees that reach down into the profile will enhance the availability of CO_2 due to bioactivity surrounding the root zones and whenever this is available then the Ca and CO_2 can precipitate $CaCO_3$ (Schmidt Mumm & Reith, 2004). This is demonstrated by the accumulations of carbonate around the root zones in the profile. Figure 6b shows root zones and their adjacent non-carbonate zones providing evidence for enhanced precipitation of carbonate and co-precipitation of Au around roots.

After examination of the data, two processes are most probably occurring concurrently to give the enrichment of Au and other metal ions. Firstly the weathering of bedrock below the dune system will incorporate minerals and elements into solution and as the water table rises due to evapotranspiration and capillary action solution will be in contact with the carbonate formation zone allowing the selective elements such as Au and Cu are incorporated into carbonate.

The extensive carbonate accumulations surrounding root zones are due to water uptake from the surrounding area. Trees in this arid environment must search for nutrients and water therefore they must have long root spans to get sufficient water to survive. These

root spans can reach down to near saprolite areas and their adjacent water reservoirs. Water that comes from near bedrock will be enriched in dissolvable elements such as Ca, Au, Mg, Al, K and Fe, as root systems draw this water upward elements are concentrated in this root zone. Due to capillary action water taken in at the root zone will draw further concentrated water upwards, continuing the process. It is also shown that concentration of elements Au, Cu, K, Al, Ca and Mg increase with depth from the surface, continuing the theory of plant root uptake any elements that are taken into roots will be transported into leaves, branches or bark and eventually deposited as biomass on the dune surface when the tree dies. Wood (1995) describes processes where humic substances dissolve and transport Au throughout soil profiles. As this biomass breaks down and its contained elements are dissolved in humic acids then the elements are going to be transported down profile. As the humic substances reach the regolith carbonate and hence Zone of Enrichment the chemical change in pH and conductivity causes metal ions to be concentrated in the precipitating carbonate phase. On site pH and conductivity taken on drill hole 1 showed great change in chemistry as the carbonate horizon was approached. Figure 2 shows the relationships developed within the soil also highlighting the enrichment of Au as the chemistry changes, which would be expected, as Au is associated with the carbonate formation.

Sequential Extraction

Assuming this is how the Au and other metal ions get into this carbonate phase examination of where the Au is situated within the sample can be undertaken. Completion of analysis from the sequential extraction showed that Au depletion is relatively even throughout the sample except when Fe oxides are removed. There are differing trends in either grain size fraction analysed. The <2μm phase clearly shows a depletion of Au when Fe and Mn oxides are removed and a weaker depletion when dolomite is removed.

Looking at the relationship between Al and K, it remains constant throughout. When there is removal of one species the other is removed proportionately. Studying the distribution after the $MgCl_2$ & acetic acid wash much more Al is removed, suggesting that the alumina species is attached more to the calcite phase or more likely that in the alumina layer of the clay Mg can substitute with Al. There is much less Au in the >2μm separate than the <2μm phase suggesting again the relationship with the <2μm clay materials and hence the association seen with Al and K. Because of the strong relationship between Au, Ca, Mg, K and Al it can be theorised that these elements all precipitate out of solution together. The results in the extraction data where the only substantial loss in Au is after application of hydroxylamine hydrochloride and hydrochloric acid suggest that although there is a strong coprecipitation relationship for the Au, carbonate and clays, dissolution is not a reversible reaction. That is however only under the current experimental procedures. It is highly likely that changing of the experimental parameters would have led to better or at least different results; the most obvious change that could be implemented is that of time of dissolution. It would be beneficial to have a larger sample so that three individual samples can be taken at each step perhaps 1hr, 12hr and 24hr could help to gain an understanding of the chemistry process. Other experimental parameters that could be implemented are a control on pH and potential oxygen values to ensure that redox reactions are not occurring and that the best possible amount of dissolution is occurring.

Sr isotopic variation

Following the sequential leach process there was analyses on various samples as to determine the possible source of the Ca within the regolith carbonates. Using $^{87}Sr/^{86}Sr$ isotope ratios results (see Table 2 and Figure 9) it is possible to deduce some of the chemistry and movement within the dune environment. Weathered granite from below the

vertical dune profile gives a value of $^{87}Sr/^{86}Sr = 0.767059\pm13$, which is supported by work completed previously in the area (Foden, 2004) (see Table 3). Sr results as high as seen here are also shown in the Himalayan river erosional zone (Oliver et al., 2003). The mass fluctuations in the data is supported by previous results (Foden, 2004), however the sample located at the surface of the dune showing a value of 1.004037±130 is not explained. Reasons for this outlier vary but most probably the result is due to the low amounts of Sr (7 ppm) in the sample give false readings in the analysis process, which did produce a large error of ±130.

Following the explanation of the more extreme results the goal for this analysis was to attempt to identify the source of the calcium. Values for samples from the dune system trench face profiles 21102, 21105, 21106, 21074 & 21114 range from $^{87}Sr/^{86}Sr = 0.716234\pm16$ at the edge of the dune to $^{87}Sr/^{86}Sr = 0.711949\pm13$ and are all quite consistent with an aeolian dune profile that has a mixing of bedrock and aeolian sources for Ca. The ratio determined for the unweathered host granite is $^{87}Sr/^{86}Sr = 0.731205\pm15$. This result can be used to compare the weathered zones and aeolian zones to aeolian influence for the Ca source. Shown by the results of samples 21102, 21105, 21106, 21074 & 21114 where the values lie much closer to that of seawater (0.7090, (Burke et al., 1982)) than that of the host granite (0.731205±15) it has to be taken that the main source for Ca within the carbonates of the dune system is sea spray. McQueen et al. (1999) suggest the Menzies Line in southeastern Australia as a marker denotes regions where the Ca source is dominated by seawater spray and Ca-rich rainfall. Lintern (2004) reports on strontium work carried out on challenger deposit and the transcontinental railway showing distance from Great Australian Bight and Sr ratio. Sr value locations from this study have the same proximity to the Great Australian Bight as Barns is and the results ($^{87}Sr/^{86}Sr = 0.7130\pm5$)

are also consistent with the Barns dune profile. Barns dune profile is not entirely dominated by aeolian marine source ($^{87}Sr/^{86}Sr_{SMOW}$ = 0.709) Ca suggesting that there is a combination of processes underway here. The isotopic data presented here imply varied sources of the Ca in carbonate such as windblown sea spray and as well as Ca derived through weathering of the granitic bedrock. Hydraulic processes such as evapo-transpiration but as demonstrated in the root zones, also plant activity play a major role in the upward transport of the Ca derived from bedrock. The mixing of the calcium (an consequently Sr) from various sources can be demonstrated by the variable Sr isotopic ratios (see Figure 9). Observations showing gradual decrease of Sr ratio the further into the dune system relates to depth from surface to sample. The further into the dune the less bedrock dominated the Sr ratio is and alternatively the nearer the edge of the dune the more bedrock dominated the ratio is. Sample 21106 located 2.5 m from surface and 4 m in from the edge is further from the bedrock source than sample 21102 which is 2.5 m from the surface but only 1 m in so is much closer to the bedrock. This could be contradicted by sample 21114 ($^{87}Sr/^{86}Sr$ = 0.714588) the root zone carbonate as it is 6 m into the dune but the value obtained is not low like 21106 ($^{87}Sr/^{86}Sr$ = 0.71194). The sample is located in a zone of water uptake from the bedrock zone by plant life so it is not an unexpected result in the sequence then it will be more strongly dominated by that bedrock than the marine source.

Conclusions

The sampling method undertaken in the project was useful as aspects of the down-hole chemistry and morphology could be studied before bulk compositions of sample were separated on lithology. The application of “real time” pH and conductivity measurements allowed the environment to be characterised chemically as well as defining the zone of

carbonate precipitation. XRF and XRD both supplied insight into the sample chemical characteristics and mineralogy of the dune system and provided data to support observations made from the trench cut through the dune. The trench revealed the internal zoning of the dune that is related to the illuvial processes that are believed to be under way in the system and not a primary sedimentary layering from the deposition of the dune. Furthermore the root zone carbonates were identified allowing theory about carbonate precipitation to be more detailed. The leach process undertaken in the project allowed some aspects of the nature of the Au to be understood. The affiliation of Au with carbonate is not reproducible, which may possibly be due to kinetic effects, such as time and temperature as well as chemical properties such as pH and Eh of the extraction procedure. However once precipitated Au is rather in metallic form and is preferentially dissolved only in strong solvents such as the combination of hydroxylamine hydrochloride and HCl at a ratio of 1:1. Finally the Sr work undertaken determined that the Ca in the samples is not derived entirely from a single source and that a combination of wind blown marine and bedrock contributes to the Ca within the dune system. However the further down the profile (i.e. the deeper the dune) the Ca is less dominated by marine aeolian sources.

Further Work

Possible areas for further study into the dune systems of Barns and other areas include a redesign of the sequential leach process that can incorporate factors such as pH and redox buffering and accounts for kinetic effects of Au solubility so a greater understanding can be achieved. Another step could be to consider the effect any humic substances will have on the chemistry of gold and carbonate. Preliminary investigations (Schmidt Mumm & Reith, 2004) have demonstrated the possible importance of biomediated carbonate precipitation in the formation of calcretes at the Barns site.

Vegetation effects on the dune system would also need to be looked into, it is a possible source for the metal ions but how much input comes from plant uptake and recycling. It also needs to be considered whether this specific case occurs elsewhere or if Barnes is unique.

Acknowledgements

I would like to thank CRC LEME for their support, my supervisor Andreas along with other staff who read my papers and offered advice with writing styles. Mark Raven of CSIRO Land and Water for assisting me with the particle separation chemistry and centrifuge as well as answering many questions I had throughout the process. John Stanley and David Bruce for their continued patience when asked about analytical techniques with XRF, XRD and mass spectroscopy. Greg Swain and Robert Dart for allowing the use of some samples needed in the strontium isotope geochemistry. All the Honours/postgraduates that offered well needed support and advice when called upon. I also need to mention Petra who has kept me focused throughout the year and given me much moral support in times of need even if it is all the way from London.

References

Beckman, G.G., 1983. Development of Old Landscapes and Soils, Soils: An Australian viewpoint, CSIRO Melbourne/ Academic Press London, pp. 51-72.

Burke, W.H., Denison, R.E., Hetherington, E.A., Koepnick, R.B., Nelson, H.F. and Otto, J.B., 1982. Variation of seawater $^{87}Sr/^{86}Sr$ throughout Phanerozoic time. Geology, 10: 516-519.

Capo, R., Stewart, B. and Chadwick, O., 1997. Sr isotopes as tracers of ecosystem processes: theory and methods. Geoderma, 82: 197-225.

Daly, S.J. and Fanning, C.M., 1993. Archaean. In: Drexel J.F., Preiss W.V. and Parker A.J. (Editors), The Geology of South Australia. Geological Society of South Australia, pp. 33-50.

Daly, S.J., Fanning, C.M. and Fairclough, M.C., 1998. Tectonic evolution and exploration potential of the Gawler Craton, South Australia. AGSO Journal of Australian Geology & Geophysics, 17(3): 145-168.

Drown, C., 2003. The Barnes Gold Project - Discovery in an emerging district. MESA, 28: 4-9.

Elburg, M. and Foden, J., 1998. Temporal changes in arc magma geochemistry, northern Sulawesi, Indonesia. Earth and Planetry Science Letters, 163: 381-398.

Ferris, G.M., Schwarz, M.P. and Heithersay, P., 2002. The geological framework , distribution and controls of Fe-oxide and related alteration, and Cu-Au mineralisation in the Gawler Craton, South Australia. Part I - Geological and tectonic framework. In: Porter T.M. (Editor), Hydrothermal iron oxide copper-gold and related deposits: A global perspective. Porter geological consultancy publishing, Adelaide, pp. 9-31.

Foden, J., 2004. Basement Sr isotope values for the Gawler Craton (unpublished work).

Foden, J., Mawby, J., Kelley, S., Turner, S. and Bruce, D., 1995. Metamorphic events in the eastern Arunta Inlier, Part 2. Nd-Sr-Ar isotopic constraints. Precambrian Research, 71: 207-227.

Gray, D.J., Wildman, J.E. and Longman, G.D., 1999. Selective and partial extraction analyses of transported overburden for gold exploration in the yilgarn Craton, Western Australia. Journal of Geochemical Exploration, 67: 51-66.

Lintern, M.J., 1989. Study and distribution of gold in soils at Mt Hope, Western Australia. Report 24R, CSIRO. Division of Exploration Geoscience.

Lintern, M.J., 1997. Calcrete sampling for gold exploration. Mesa, 5: 5-8.

Lintern, M.J., 2004. The South Australian regolith project final report - Summary and Synthesis. CRC LEME Open file report, 156: 120-121.

McLean, M.A. and Betts, P.G., 2003. Geophysical constraints of shear zones and geometry of the Hiltaba Suite granites in the western Gawler Craton, Australia. Australian Journal of Earth Sciences, 50(4): 525-541.

McQueen, K.G., Hill, S.M. and Foster, K.A., 1999. The nature and distribution of regolith carbonate accumulations in southeastern Australia and their potential as a sampling medium in geochemical exploration. Journal of Geochemical Exploration, 67: 67-82.

Moore, D.M. and Reynolds, R.C., 1989. X-ray Diffraction and the Identification and Analysis of Clay Minerals. Oxford Press.

Oliver, L., Harris, N., Bickle, M., Chapman, H., Dise, N. and Hortswood, M., 2003. Silicate weathering rates decoupled from the $^{87}Sr/^{86}Sr$ ratio of the dissolved load during Himalayan erosion. Chemical Geology, 201: 119-139.

Potts, P.J., 1992. X-ray fluorescence analysis: Principles and practice of wavelength dispersive spectrometry. In: Blackie (Editor), A Handbook of Silicate Rock Analysis., London, pp. 226-285.

Rayment, G.E. and Higginson, F.R., 1992. Australian laboratory handbook of soil and water chemical methods. Australian soil and land survey handbooks, 3. inkata press, Melbourne.

Schmidt Mumm, A. and Reith, F., 2004. Biogeochemistry of calcrete forming processes. Advances in regolith; proceedings of the CRC LEME regional regolith symposia

2004. Cooperative Research Centre for Landscape Environments and Mineral Exploration., Bentley, West. Aust., Australia.

Sietronics, 2004. SIROQUANT - Quantitative Powder XRD Phase Analysis Software for Windows (www.sietronics.com.au).

Stewart, B., Capo, R. and Chadwick, O., 1997. Quantitative strontium isotope models for weathering, pedogenesis and biogeochemical cycling. Geoderma, 82: 173-195.

Tessier, A., Campbell, P.G.C. and Bisson, M., 1979. Sequential extraction procedure for the speciation of particulate trace metals. Analytical Chemistry, 51(7): 844-851.

Thomson, B.P., 1975. Gawler Craton, South Australia. Economic geology of Australia and Papua New Guinea, 1, Metals. Australasian Institute of Mining and Metallurgy, 461-466 pp.

Wood, S.A., 1995. The role of humic substances in the transport and fixation of metals of economic interest (Au, Pt, Pd, U, V). Ore Geology Reviews, 11: 1-31.

Table 1.

a)

Sample number	21001	21002	21003	21004	21005	21006	Error
Depth(m)	0-0.3	0.3-0.6	0.6-1.0	1.0-1.3	1.3-1.5	1.5-1.95	
Quartz	7	4	4	6	4	4	1
Kaolin	48	42	46	50	46	39	5
Smectite	38	48	44	37	40	47	5
Anatase	1	1	1	1	1	<1	1
Goethite	<1	<1	<1	<1	1	1	1
Mica	6	5	5	5	7	4	1
Dolomite	-	-	-	-	-	6	1
Total	100	100	100	99	99	101	

b)

	21001	21002	21003	21004	21005	21006
>2µm weight	19.20	19.58	19.49	21.18	18.90	16.80
<2µm weight	0.57	1.13	1.63	0.59	1.77	4.06
Wt% Clay per sample	2.88	5.46	7.72	2.71	8.57	19.45
Total Wt% Kaolin	1.38	2.29	3.55	1.36	3.94	7.59
Total Wt% Smectite	1.09	2.62	3.40	1.00	3.43	9.14

Table 1a) Wt% of <2um grain size in each sample after grain size separation increasing with depth
b) Quantitative estimates of clay mineral contents based on the SIROQUANT program (Sietronics 2004)

Table 2.

Sample.	Location	Sr^{87}/Sr^{86} ratio
21071	Top of eastern face vertical profile	1.004037±130
21102	1.0m into dune eastern face from southern edge at 2.5m depth from surface	0.716234±16
21105	3.5m into dune eastern face from southern edge at 2.5m depth from surface	0.713616±13
21106	4.0m into dune eastern face from southern edge at 2.5m depth from surface	0.711949±13
21074	Bottom of eastern face vertical profile 3.2m from southern edge and 3.5m depth	0.715379±12
21114	Root carbonate 6m into dune from southern edge at 3.5m depth from surface	0.714588±12
BA04	Under dune weathered and silicified saprolite	0.767059±13
21118	Drill hole of highly weathered granite	1.068547±16
BNS Granite	Drill core of fresh bams granite at depth	0.731205±15
Foden 1	Paragneiss, Westren Eyre peninsula	1.012600±4
Foden 2	Kiana Granite Pt Drummond	0.911659±28
Foden 3	Coulta Granite Pt Drummond	0.762447±18
	Indicates data taken from Foden, (2004)	

Table 2) Whole rock $^{87}Sr/^{86}Sr$ ratios for samples of dune material and bedrock on the Barns prospect

Figure Captions

Figure 1a) Site location of fieldwork inset Australian map showing location. Geology adapted from Drown (2003) b) Barnes Au project showing trench and hole location for analyses.

Figure 2) Plot of pH, conductivity and Au concentration through hole 1.

Figure 3) a) Au to metal oxide relationships in the depth profile of the initial drill hole, note the distinct co-variation of Au with the metal oxides. b) Correlation of major elements and Au in the drilled profile showing trendlines of each metal oxide to Au.

Figure4a) Vertical profile of western face of the trench showing concentration of metal oxides in Wt%, Au and Cu in ppb and ppm respectively, note the correlation between CaO, K_2O and Au. b) Vertical profile of eastern face of trench in dune c) Horizontal profile of trench face

Figure 5a) Eastern face of trench showing sample locations and interpretation from field observations of internal differentiation of the dune

Figure 6a) Depth vs. concentration plot through vertical profile of eastern face of dune highlighting the area of enrichment seen in figure 4a. b) Plot showing metal oxide weight percentages from root zone carbonates against non-root zone carbonates within proximity of each other highlighting the relationship of Au with calcite in the root zones.

Figure 7a) Plot of data from drill hole 1 showing elemental concentration changes relative to the depositional surface. Highlighting the strong increase in concentration of Ca, Al, K and Mg. Vertical line denotes the most recent material at the top of the profile. The x-axis shows the value of the recent surface materia then each further value is plotted against this surface value. Points above the line represent an increase in concentration of elements with respect to the surface and points below the line indicate a decrease in concentration of elements with depth. Samples have been made relative to each other by division of original values allowing the data to be plotted on the same axis. b) Plot following same method however data used is from vertical profile on the eastern face of the dune trench.

Figure 8a) <2μm fraction from sequential process showing results of whole rock ICP – MS and OES following each step of the partial extraction, highlighting relationships between Al, Au, Ca, Cu, K, Mg, Mn & Zr. As in figure 7, x-axis shows the value of the untreated sample and the following samples are plotted against this sample. b) >2μm fraction results from sequential leach process following the same process.

Figure 9 Results from $^{87}Sr/^{86}Sr$ shown in Table 2 plotted to show distribution of each sample and sample results from Foden (2004) demonstrating that results such as the ones seen in the paper exist in the area.

Figures

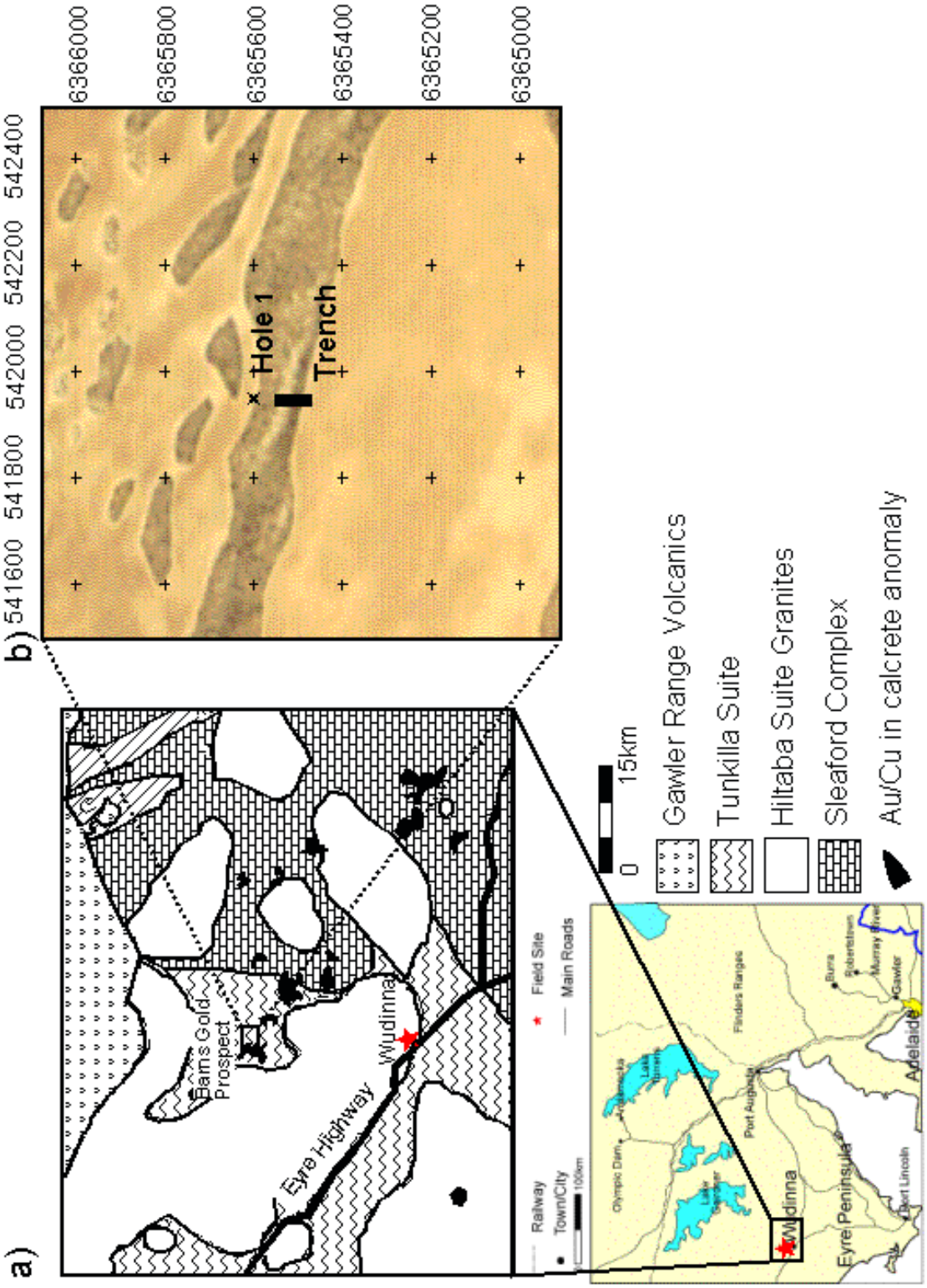

Figure 1.

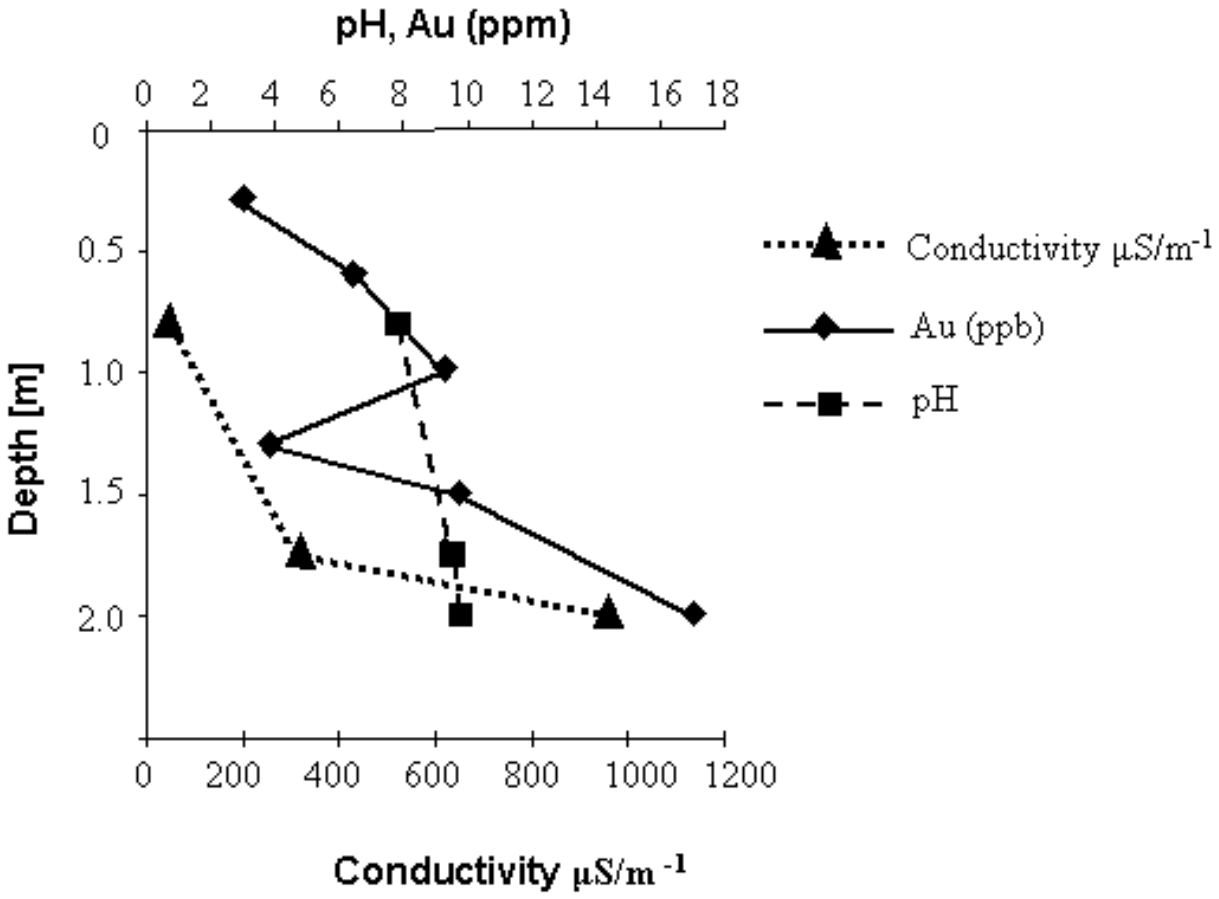
pH, Au (ppm)
0 2 4 6 8 10 12 14 16 18
0
0.5
1.0
1.5
2.0
Depth [m]
0 200 400 600 800 1000 1200
Conductivity µS/m -1
Conductivity µS/m-1
Au (ppb)
pH

Figure 2.

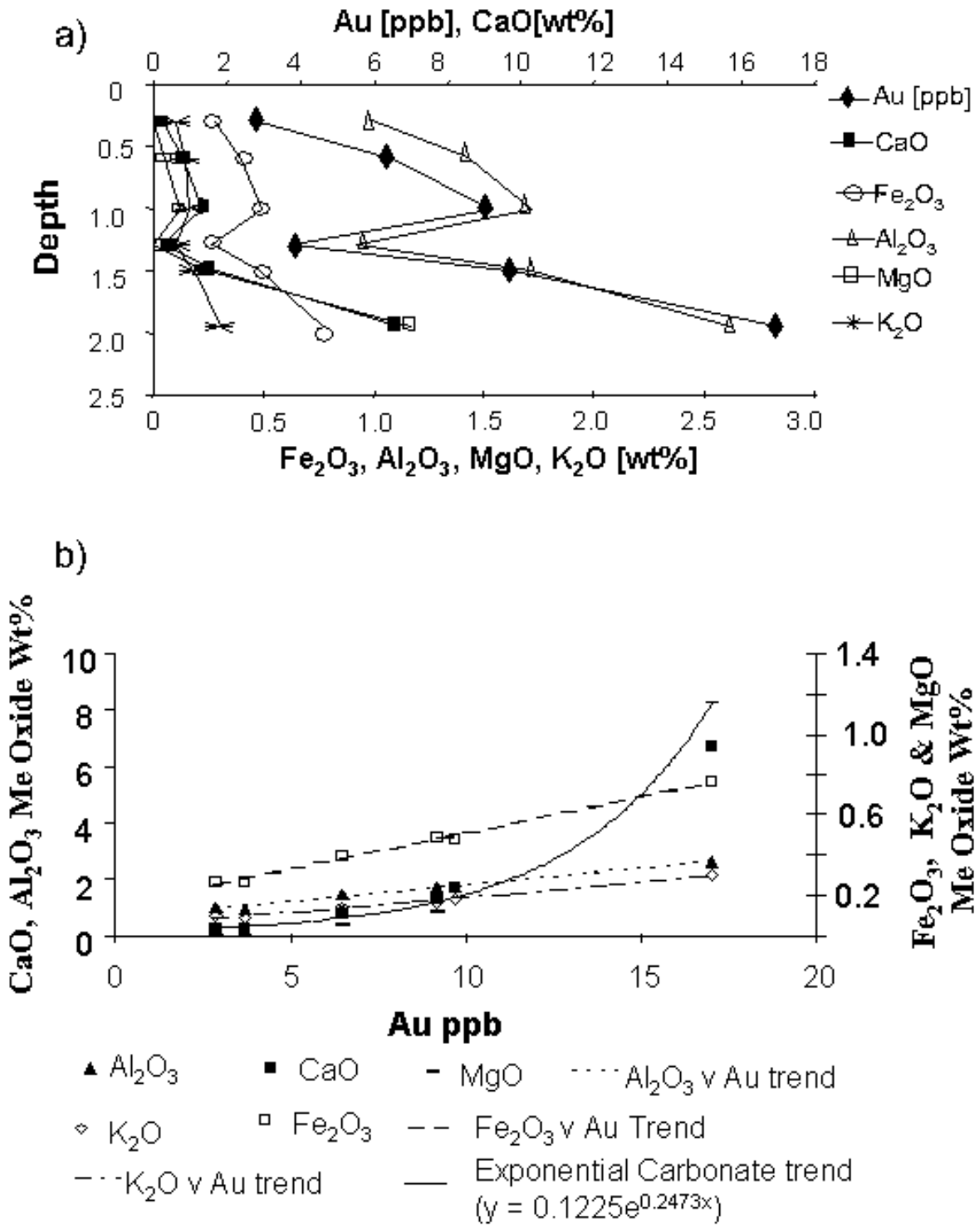
a)
Au [ppb], CaO[wt%]
Depth
Fe2O3, Al2O3, MgO, K2O [wt%]
Au [ppb]
CaO
Fe2O3
Al2O3
MgO
K2O
b)
CaO, Al2O3 Me Oxide Wt%
Fe2O3, K2O & MgO Me Oxide Wt%
Au ppb
Al2O3
CaO
MgO
Al2O3 v Au trend
K2O
Fe2O3
Fe2O3 v Au Trend
K2O v Au trend
Exponential Carbonate trend
(y = 0.1225e0.2473x)

Figure 3.

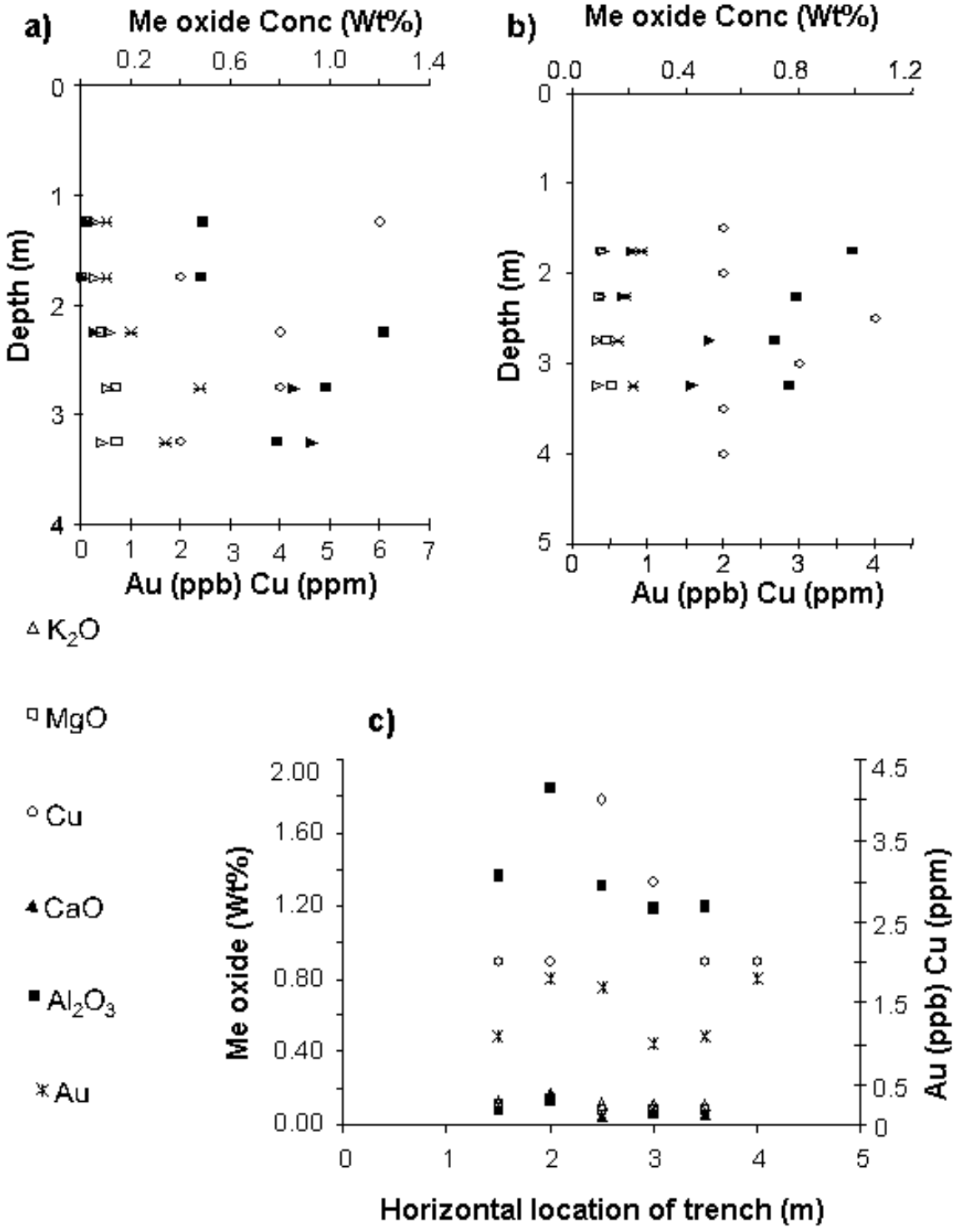
a)
Me oxide Conc (Wt%)
0.2
0.6
1.0
1.4
Depth (m)
Au (ppb) Cu (ppm)
b)
Me oxide Conc (Wt%)
0.0
0.4
0.8
1.2
Depth (m)
Au (ppb) Cu (ppm)
K2O
MgO
Cu
CaO
Al2O3
Au
c)
Me oxide (Wt%)
Au (ppb) Cu (ppm)
Horizontal location of trench (m)

Figure 4.

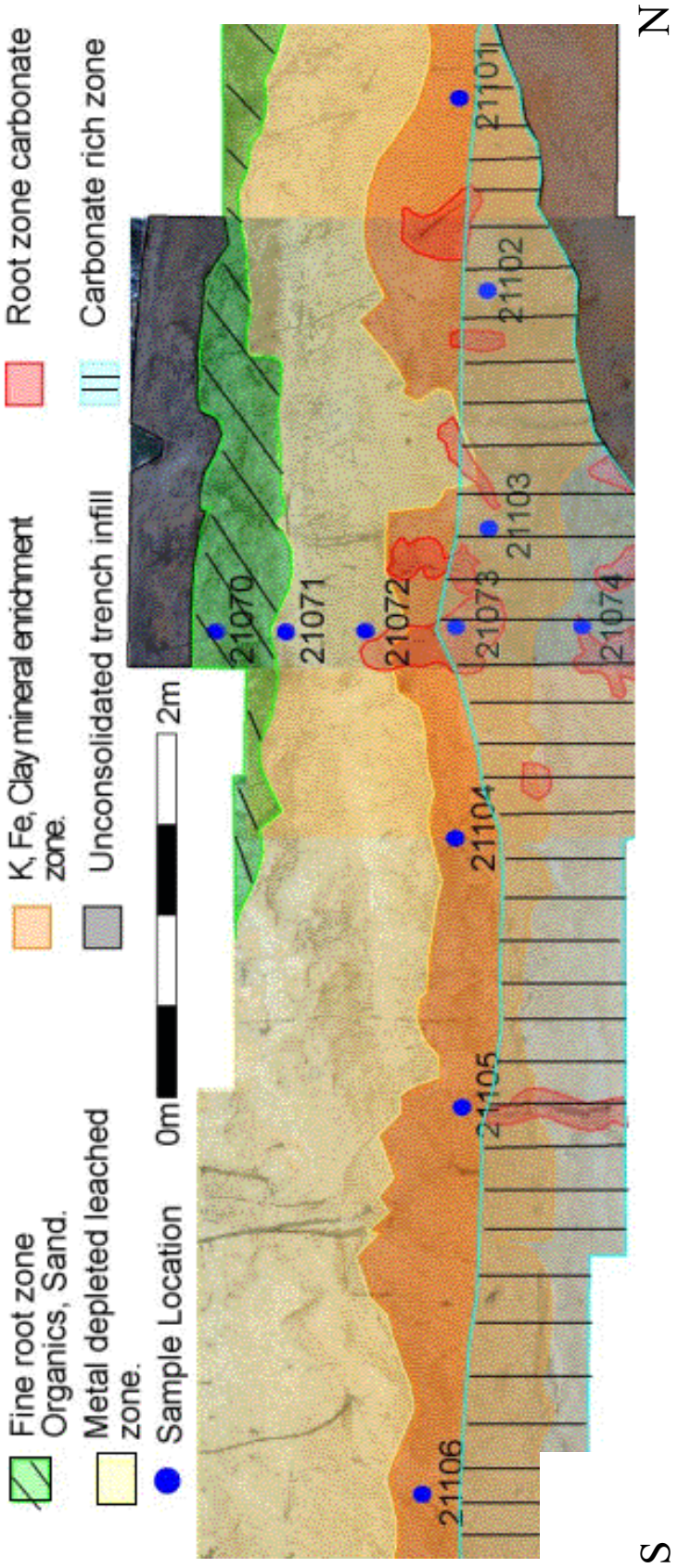
Root zone carbonate
Carbonate rich zone
K, Fe, Clay mineral enrichment zone.
Unconsolidated trench infill
Fine root zone Organics, Sand.
Metal depleted leached zone.
Sample Location
0m
2m
N
S
21070
21071
21072
21073
21074
21101
21102
21103
21104
21105
21106

Figure 5.

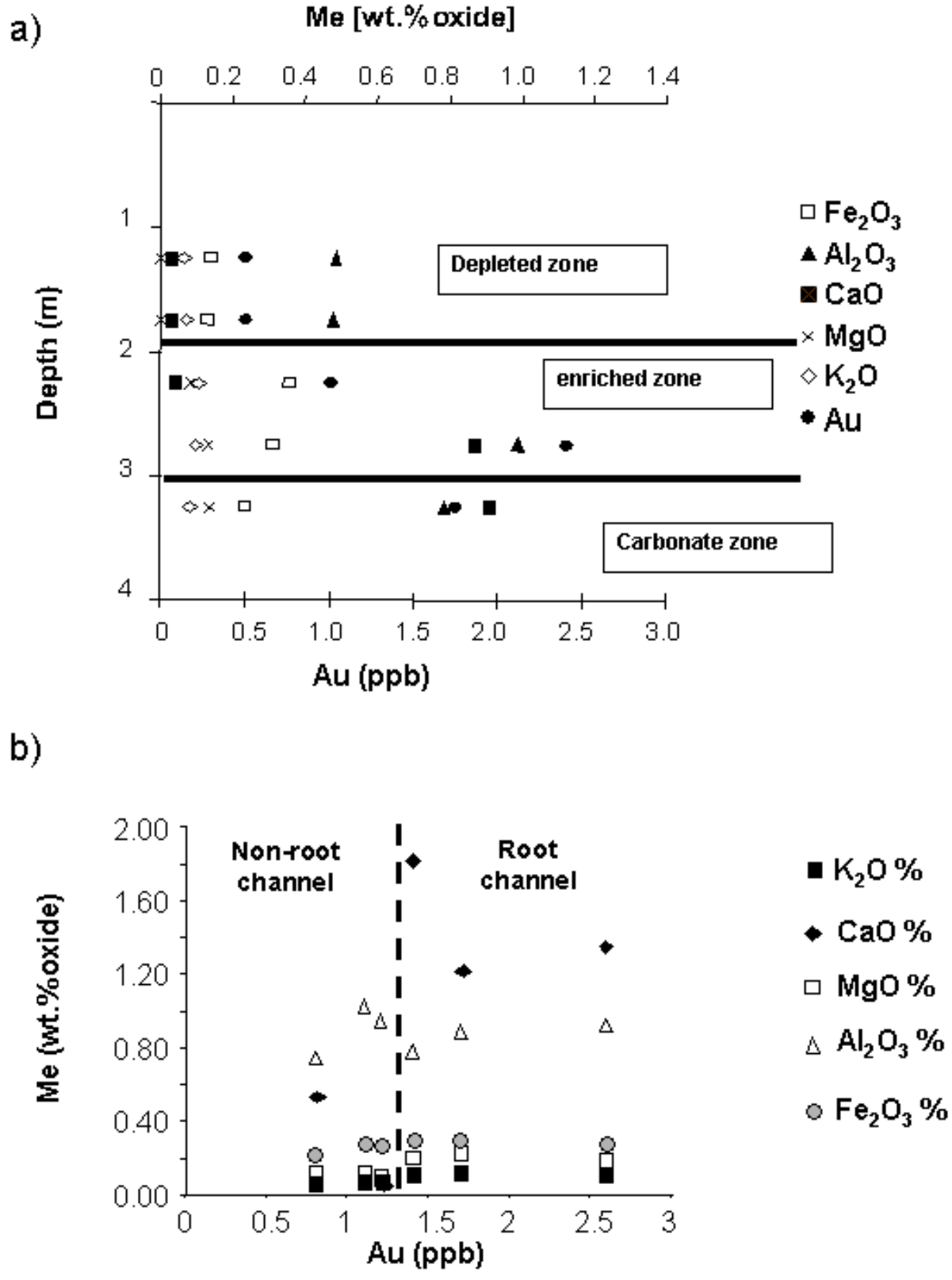
a)
Me [wt.% oxide]
0 0.2 0.4 0.6 0.8 1.0 1.2 1.4
Depth (m)
1
2
3
4
Depleted zone
enriched zone
Carbonate zone
Fe2O3
Al2O3
CaO
MgO
K2O
Au
0 0.5 1.0 1.5 2.0 2.5 3.0
Au (ppb)
b)
Me (wt.%oxide)
2.00
1.60
1.20
0.80
0.40
0.00
Non-root channel
Root channel
0 0.5 1 1.5 2 2.5 3
Au (ppb)
K2O %
CaO %
MgO %
Al2O3 %
Fe2O3 %

Figure 6.

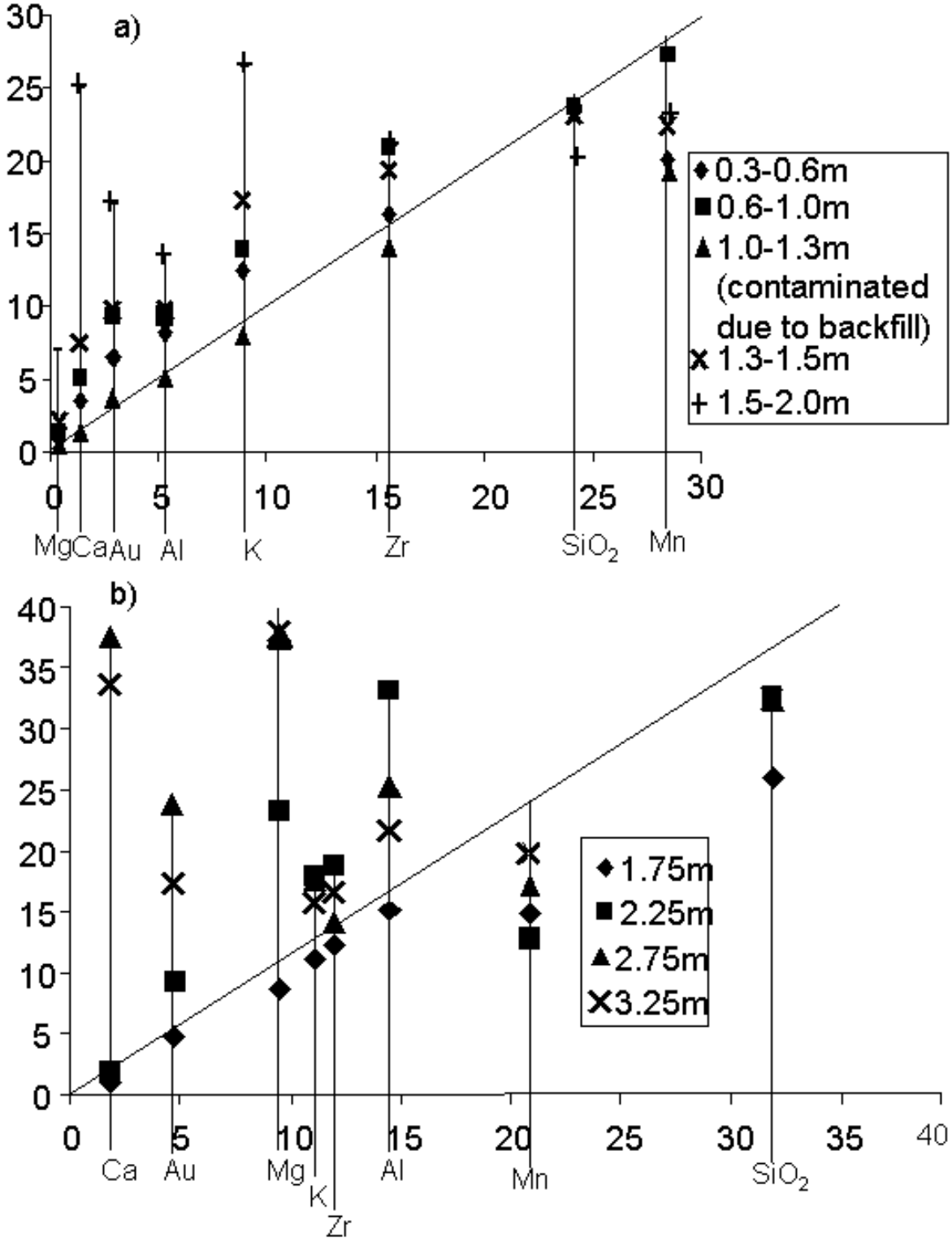
a)
0.3-0.6m
0.6-1.0m
1.0-1.3m (contaminated due to backfill)
1.3-1.5m
1.5-2.0m
Mg
Ca
Au
Al
K
Zr
SiO2
Mn
b)
1.75m
2.25m
2.75m
3.25m
Ca
Au
Mg
K
Zr
Al
Mn
SiO2

Figure 7.

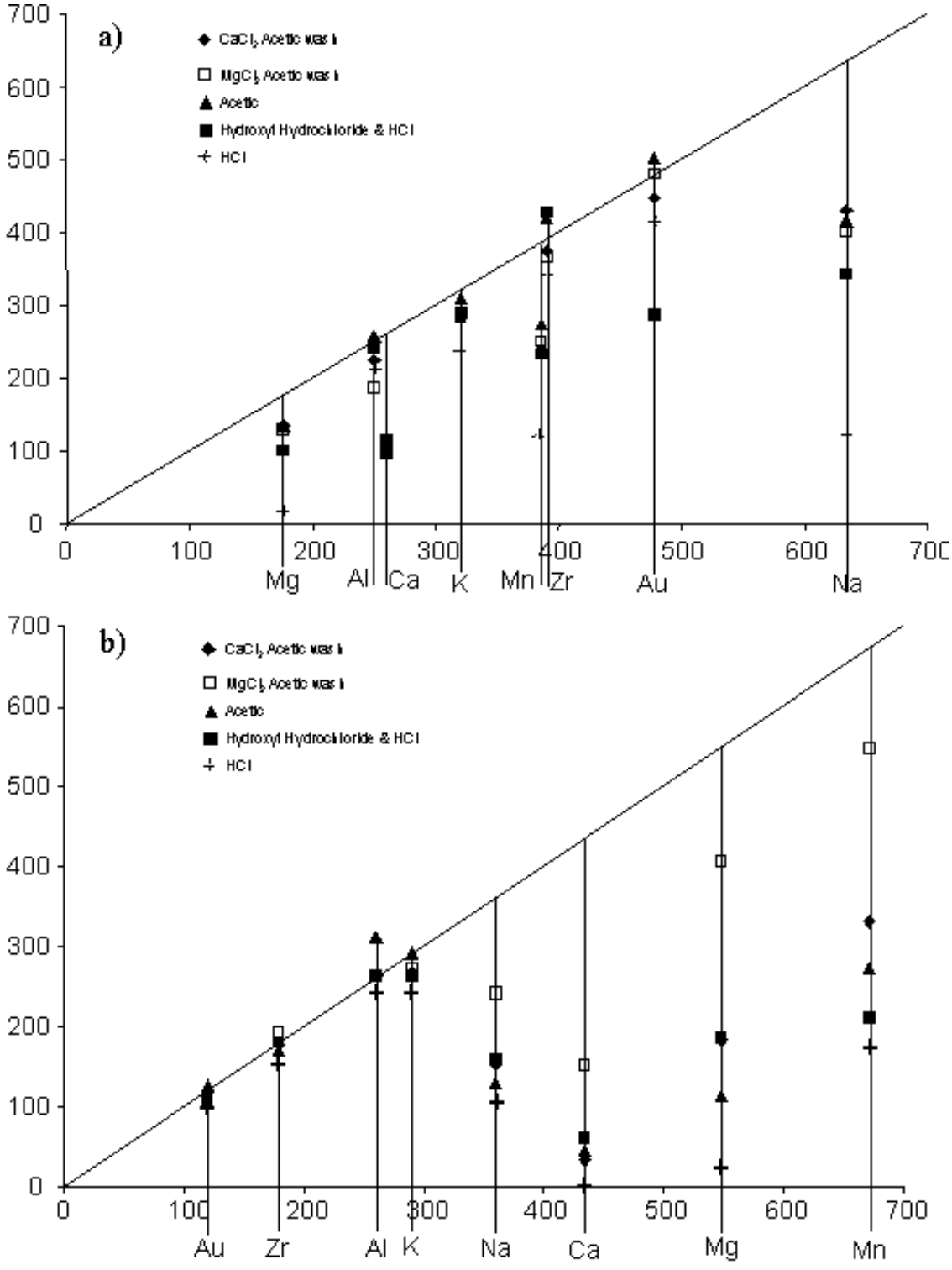
a)
CaCl2 Acetic wash
MgCl2 Acetic wash
Acetic
Hydroxyl Hydrochloride & HCl
HCl
700
600
500
400
300
200
100
0
0
100
200
300
400
500
600
700
Mg
Al
Ca
K
Mn
Zr
Au
Na
b)
CaCl2 Acetic wash
MgCl2 Acetic wash
Acetic
Hydroxyl Hydrochloride & HCl
HCl
700
600
500
400
300
200
100
0
0
100
200
300
400
500
600
700
Au
Zr
Al
K
Na
Ca
Mg
Mn

Figure 8.

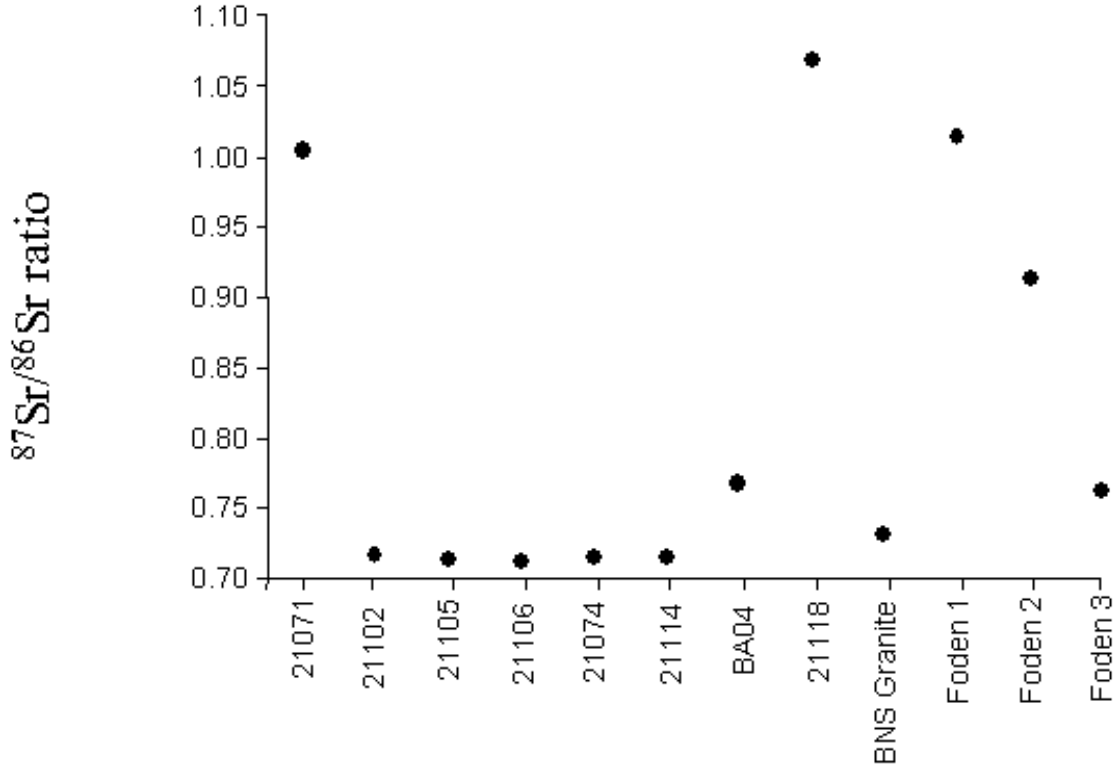
$^{87}Sr/^{86}Sr$ ratio
1.10
1.05
1.00
0.95
0.90
0.85
0.80
0.75
0.70
21071
21102
21105
21106
21074
21114
BA04
21118
BNS Granite
Foden 1
Foden 2
Foden 3

Figure 9.